



Electrophysical Response of Soil to Changes in Moisture

**Farxod Turgunboev*, Kamiljan A. Tursunmetov, Feruza A. Giyasova, Murodjon A. Yuldoshev,
Farkhod A. Giyasov, Azimjon A. Abduvakhobov, Alisher A. Mamadaliyev**

Assistant Professor, PhD, National University of Uzbekistan named after Mirzo Ulugbek, Tashkent, Uzbekistan

Professor, DSc, National University of Uzbekistan named after Mirzo Ulugbek, Tashkent, Uzbekistan

Professor, DSc, Kimyo International University in Tashkent, Uzbekistan

Assistant Professor, PhD, Turan International University, Namangan, Uzbekistan

Head teacher, Kimyo International University in Tashkent, Uzbekistan

Head teacher, Kimyo International University in Tashkent, Uzbekistan

Master's student, Kimyo International University in Tashkent, Uzbekistan

ABSTRACT: This paper examines the electrophysical parameters of the main soil types in the Tashkent and Syrdarya regions (sierozems, loams, and fine- and coarse-grained sands) over a moisture content range of 5-30 % and frequencies up to 100 kHz. Electrical resistivity measurements were conducted using a specially designed cell and controlled moisture conditions. It was found that soil resistivity decreases with increasing moisture content, with the sharpest decrease observed at low ω values (up to 12-15 %), corresponding to aqueous phase percolation. At high frequencies ($\geq 10^4$ Hz), the contribution of electrode and volume polarization decreases, and electrical conductivity is determined primarily by the ionic conductivity of the pore solution. The frequency dispersion of resistivity is pronounced at low moisture contents and low frequencies, whereas at saturation ($\omega > 20$ %), the curves for different frequencies converge. It has been shown that particle size distribution significantly influences the electrophysical response: coarse-grained sands exhibit the highest ρ values, while loams exhibit the lowest. The results allow for the refinement of soil conductivity models that take into account frequency and moisture-dependent effects and can be used in developing methods for electrophysical monitoring of soil moisture and geotechnical properties.

KEY WORDS: Soil resistivity, electrical conductivity, soil moisture, frequency dispersion, sierozems, loams, sandy soils, alternating current, geotechnical properties.

I. INTRODUCTION

A modern trend in crop production is the implementation of precision farming technologies, based on the differentiated application of fertilizers based on spatial heterogeneity of soil fertility. To ensure agrochemical assessment that meets cost-effectiveness and efficiency requirements, the development of highly accurate analytical methods is a pressing issue. One such approach is the electrophysical method [1, 2], based on measuring electrical resistance, which has become widely used in soil analysis. Application of this method has confirmed its practical value as an effective and quickly implemented approach to comprehensive soil characterization.

Soil moisture is one of the key factors determining plant growth and development [3,4]. Therefore, its determination and control are of fundamental importance. Assessing soil fertility, taking into account the spatial and genetic heterogeneity of soil properties, is a labor-intensive task requiring the collection of a large number of samples and their subsequent analysis in laboratory conditions. However, in some cases, when characterizing the soil cover, it is sufficient to determine the degree of expression of one or more indicators reflecting the genetic specificity of the soil [5, 6]. An effective solution to this problem contributes to the development and implementation of methods that allow for direct measurements of integral parameters reflecting a set of key soil properties or its basic characteristics used to assess its condition. One such parameter can be the specific electrical resistance of the soil, determined both in laboratory and in the field [7, 8]. A significant feature of this indicator is its high sensitivity to a wide range of factors [9-11].

In the current context, measurement methods in direct and alternating electric fields are used to determine the electrical characteristics of soils, each with its own advantages and limitations. The key criterion for choosing a method is the ability to obtain the most complete information about the properties of the object under study. The most technologically advanced approach is considered to be conducting measurements in alternating current,



taking into account its frequency characteristics [12]. However, in our opinion, insufficient attention has been paid to the frequency dependence of measurement results when studying parameters such as the specific electrical resistance of the soil. In our previously published work [13], as well as in a number of other studies [14, 15], the electrical properties of soil were studied depending on its moisture content, including the region of tightly bound moisture in the frequency range of 20 - 200 kHz [16]. It was found that with increasing frequency, a decrease in the specific electrical resistance and relative permittivity of the soil is observed. In addition, the dependence of the real and imaginary parts of the complex permittivity on soil moisture was investigated in [17] using a capacitive method at a frequency of 50 MHz and a “Hadro probe” sensor. The results of the study indicate that with increasing soil moisture, both the real and imaginary components of the permittivity increase.

The aim of this work is to obtain and evaluate data on the degree of influence of the frequency of the electrical signal on the values of measured specific electrical resistance against the background of changes in the soil moisture index.

II. EXPERIMENTAL SAMPLES AND MEASUREMENT METHODS

To study the influence of various factors on the electrophysical parameters of the main soil types in the Tashkent and Syrdarya regions of the Republic of Uzbekistan, sierozems and ordinary alluvial soils were selected. Using these soil types, a study was conducted on the electrophysical response of the soil to changes in moisture content. Sampling was carried out in areas not used for agricultural production.

Electrical resistance measurements were performed in the laboratory after humidifying the samples. The following parameters were determined: humidity using thermostatic gravimetric analysis, temperature using a Brymen BM257 digital multimeter, and electrical resistance using a GZ-109 measuring instrument-generator, which provides a sinusoidal output signal with a frequency of up to 100 kHz, high power, and precise frequency and amplitude adjustment. For direct measurements, specially designed electrodes were used, consisting of copper plates, a glass cuboid vessel without a top face, a metal base, and a shield to protect against external electromagnetic interference. The outgoing wires were also shielded.

A total of over 50 soil samples were collected in the field. Electrical resistance was measured both horizontally and vertically at the sampling points, providing a comprehensive assessment of the distribution of soil electrical properties.

In the course of the experiment, four types of soil samples differing in granulometric composition were studied: crushed and sieved soil with particle sizes $d \leq 1$ mm, granulated loams with particle sizes up to 3 - 4 mm, fine-grained sand with a clay content of about 30%, and coarse-grained alluvial sand from the SyrDarya riverbed with particle sizes in the range $d \leq 0.1 - 1$ mm. Sample preparation was carried out according to a unified procedure: the soil of the first group was dried to an air-dry state and sieved through a mesh with a cell size of about $d \approx 1$ mm, ensuring uniform composition, while the samples of the second group were subjected to natural drying in the open air for one month, after which they were crushed to a granulated structure. The sandy soil samples were used in their natural state with preliminary control of silt and clay fractions. For measurements, a 1 kg portion of each material type was taken and placed in cylindrical plastic containers with a diameter of about 10 cm, which ensured uniform placement and packing density, as well as comparability of the obtained results.

The measurements of electrophysical parameters were carried out using specially fabricated stainless steel electrodes designed as flat plates with a width of 2 cm. The electrodes were fastened with screw connections, which ensured reliable electrical contact when connected to the power source. The use of stainless steel as the electrode material made it possible to eliminate corrosion processes during long-term operation (over 3000 hours) and, consequently, to avoid additional systematic errors associated with changes in contact characteristics. The electrodes were immersed in the soil samples to a depth of 10–12 cm, while the interelectrode spacing was fixed at 2 cm. This geometry of the measuring cell ensured reproducibility of the experimental conditions and the accuracy of comparing the results obtained across different measurement series.

In order to ensure metrological reliability, special attention was paid to error control:

- the dimensions of the electrodes were maintained with a tolerance of ± 0.1 mm;
- the sample weight was controlled by analytical scales with an error of no more than ± 0.01 g;
- compaction of samples was carried out using a single method, ensuring the same density in all series of experiments;

- Temperature and humidity conditions in the room were recorded, reducing the influence of external factors on the results. This set of measures minimized systematic and random errors and ensured high reproducibility of the obtained data.

According to literary sources [18, 19], soil electrical conductivity depends significantly on its moisture content, as water in the soil pores facilitates ion transport. One informative method for analyzing soil conductivity is to measure the volt-ampere characteristic, which reflects the dependence of current strength on the applied voltage. The electrical circuit was assembled according to the following scheme (see Fig. 1): Power supply (DC or AC) → DC/AC switch → Soil sample with electrodes → Measuring instruments (depending on the mode) → Monitoring of parameter changes under varying soil moisture conditions. The voltmeter was connected in parallel to the electrodes. The voltage was varied from 0 to 40 V in steps of 0.5 V. At each step, the values of voltage (U) and current (I) were recorded. The measurements were carried out at a constant temperature of 25 ± 1 °C.

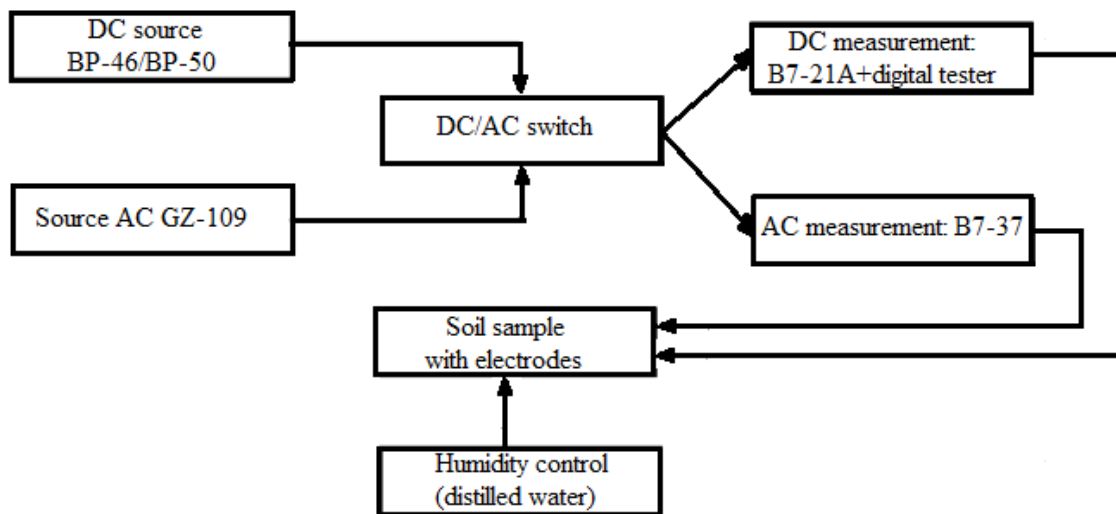


Fig. 1. Block diagram for the soil conductivity measurement setup

A DC power supply of the BP-46/BP-50 type was used to apply voltage to the electrodes; voltage and current measurements were performed using a V7-21A voltmeter with additional control by a digital tester. In studies under AC conditions, the voltage was generated by a GZ-109 generator, and the current was recorded using a V7-37 voltmeter. Soil moisture was regulated by adding distilled water, calculated by mass.

The obtained current–voltage characteristics (I–V curves) under DC voltage in the range of 0–40 V exhibited a linear behavior up to a moisture content of 30% [13]. Similar results were recorded under AC excitation in the frequency range of 20–100 Hz: the I–V curves remained linear, and the values of specific resistance coincided with those determined by the DC method. Therefore, the specific resistance measured at a frequency of 100 Hz can be considered equivalent to the resistance obtained under direct current.

III. EXPERIMENTAL RESULTS AND DISCUSSION

Experimental data were obtained over a moisture content range of 5-30%. Specific resistance was determined over a frequency range of 10-100 kHz, allowing for an assessment of the frequency dependence of the samples' electrical conductivity. Specific resistance measurements under alternating current were performed over a range of effective voltage values of 1-4 V. Soil resistivity at various moisture levels was determined using the formula:

$$\rho = [(I/U) S]/d \text{ or } \rho = RS/d, \tag{1}$$

where, U is the applied voltage, I is the current, S is the area of the electrode plate, d is the distance between the electrodes, R is the soil resistance for a given sample.

To ensure metrological reliability, each measurement was performed in triplicate, and the results were averaged. An assessment of the measurement error showed that it did not exceed $\pm (2\div 3)$ % of the measured resistivity value. Furthermore, to determine the specific electrical resistance of moist soil and ensure high accuracy of the obtained

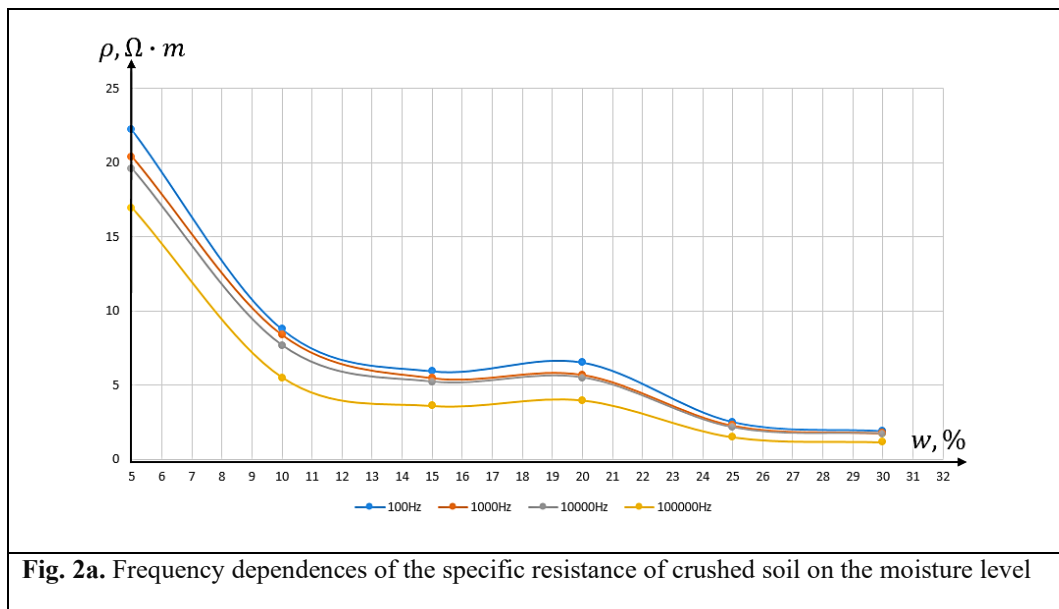
data, a series of measurements were performed in which signals of different frequencies were applied and changes in the resistance of the samples were recorded. An empirical model based on the Archie's Law equation [20] was used to interpret the experimental results.

$$\rho = a \rho_w (\Phi/\Phi_0)^{-m}, \tag{2}$$

$$\rho(f) = \rho_0 f^\alpha \tag{3}$$

where, ρ is the specific resistivity of the soil, ρ_w is the specific resistivity of water, a is an empirical coefficient (depending on soil type), Φ is the soil porosity, Φ_0 is the maximum porosity, m is a coefficient accounting for the influence of porosity on conductivity, ρ_0 is the specific resistivity at frequency f_0 , and α is a coefficient reflecting the influence of soil granulometric composition and its degree of moisture.

It is known that the specific electrical resistance of the soil (ρ) is an integral parameter reflecting the combined influence of its moisture content, salt composition and structural features, which makes it one of the key indicators of the electrophysical properties of the soil environment [21, 22]. Figure 2a shows the curves of the dependence of the specific resistance ρ on moisture content for crushed soil at different frequencies (100-100 kHz).



The experimental form of the curves is well approximated by an exponential or power law [23] of decrease, for example:

$$\rho(\omega, f) \approx \rho_0(f) \exp(-k(f)\omega), \tag{4}$$

where the coefficients $\rho_0(f)$ and $k(f)$ depend on frequency (ρ_0 decreases with increasing f , while k may also vary). Parameter fitting using the least squares method makes it possible to quantitatively describe the frequency dispersion. From Fig. 2a it should be noted that on the horizontal axis the volumetric soil moisture ω (%) is plotted, while on the vertical axis the specific electrical resistivity ρ ($\Omega \cdot m$) is shown. For four frequency values (100, 10^3 , 10^4 , and 10^5 Hz), the dependencies $\rho(\omega)$ were constructed. Analysis of the obtained data allows the following regularities to be identified [24, 25]:

- A monotonic decrease in the specific resistivity of the soil is clearly observed in the moisture range from 5 to 20%: at $\omega \approx 5\%$, the values reach 30–35 $\Omega \cdot m$, whereas at $\omega \approx 20\%$ the resistivity decreases to the level of 4–5 $\Omega \cdot m$, indicating the dominant contribution of ionic conductivity under conditions of increased moisture content;
- The nonlinearity of the $\rho(\omega)$ dependence is manifested in the fact that at low moisture levels the decrease in specific resistivity occurs most sharply, forming a steep section of the curve, whereas with a further increase in ω the rate of resistivity reduction slows significantly, and the dependence acquires a quasi-linear character;
- The presence of pronounced frequency dispersion: at a fixed moisture content, the specific resistivity systematically decreases with increasing frequency ($\rho(100 \text{ Hz}) \geq \rho(10^3 \text{ Hz}) \geq \rho(10^4 \text{ Hz}) \geq \rho(10^5 \text{ Hz})$). This effect

is caused by polarization processes and reflects the characteristic frequency dependence of the electrical conductivity of the soil medium;

- In the region of high moisture content ($\omega \approx 20\%$), the differences between the dependencies obtained at various frequencies become minimal. This indicates that the electrical conductivity is determined primarily by the ionic conductivity of the pore solution, while the influence of surface and polarization processes is significantly reduced.

The shape of the obtained dependencies (Fig. 2a) is rather complex; however, a general trend is observed in all cases—namely, a decrease in specific resistivity with increasing moisture content. As moisture increases, the specific resistivity of the soil decreases across the entire frequency range. This is explained by the growth of ionic conductivity due to the increased amount of free water, dissolved salts, and improved ion transport in the pores. At low frequencies (100–1 kHz), the specific resistivity is higher, which is associated with pronounced polarization effects [26] at the electrode–soil interface and the slow redistribution of ions. At high frequencies (10^4 – 10^5 Hz), water dipoles and ionic clouds cannot follow the alternating field, and therefore the polarization contribution decreases, resulting in lower resistivity. In the range of $\omega \approx 20\%$, the differences between the curves are reduced, indicating a transition to the saturated conductivity regime. In this case, the main mechanism becomes bulk ionic conductivity of the liquid phase [27], which is less dependent on frequency. The dependence of specific resistivity on moisture content is nonlinear and strongly determined by the measurement frequency.

It is evident that the electrical resistivity of soil is formed under the influence of several mechanisms, whose contribution varies with the frequency of the electric field and the moisture content. The specific electrical resistivity of soil is determined by the combined action of these mechanisms, with their relative influence depending on the frequency of the electric field and the level of moisture [28].

Based on the experimental data presented in Fig. 2a, an annotated graph (Fig. 2b) was constructed, illustrating the variation of soil resistivity as a function of moisture content at different frequencies. The graph highlights key regions and the corresponding mechanisms that govern the system’s behavior.

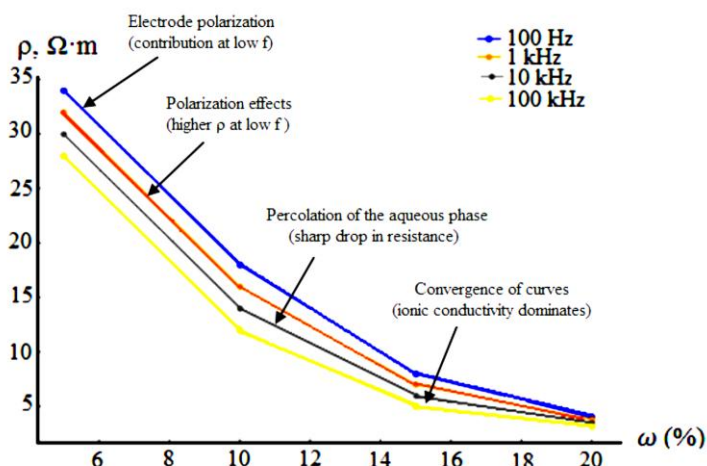


Fig. 2b. Annotated dependence $\rho(\omega)$ for soil in the frequency range 100 Hz – 100 kHz

From Fig. 2b it can be seen that at low frequencies, electrode polarization [29] occurs in the system, leading to a significant increase in the measured resistivity due to the formation of a double electric layer at the “electrode–soil” interface. In the low-frequency region (about 100–1000 Hz), the formation of this double electric layer at the electrode–soil boundary has a considerable effect. This process results in additional resistance due to charge accumulation at the contact interfaces. As a consequence, the measured values of specific resistivity are overestimated. This effect is most pronounced at low moisture levels, when the ion concentration in the pore fluid is minimal and charge transport is hindered. In addition to electrode polarization, bulk polarization effects [30, 31] are also observed at low frequencies, caused by the heterogeneity of the soil matrix. The difference in dielectric properties of the solid phase and the pore fluid induces interfacial polarization of the Maxwell–Wagner type [32, 33].

As the frequency increases, these processes gradually weaken: the relaxation time of charges becomes shorter, and the system no longer has time to form pronounced polarization layers. As a result, the contribution of polarization decreases, and the specific resistivity begins to be determined mainly by bulk conductivity. With increasing moisture, a sharp drop in specific resistivity is observed, which is associated with percolation processes

of the water phase [34]. The filling of capillaries and micropores with water leads to the formation of a continuous network of conductive channels through which effective ion transport occurs. This process is nonlinear: once a critical moisture threshold is reached, even a small addition of water causes a multiple reduction in resistivity. Under conditions of significant soil saturation with moisture, the resistivity–frequency curves become almost identical. This indicates that the main charge transport mechanism is the ionic conductivity [35, 36] of the solution filling the pore space. In these conditions, the contribution of electrode and bulk polarization is minimal, and the electrical characteristics of the system are primarily determined by the concentration of dissolved salts and the degree of water saturation.

Next, Fig. 2c shows the specific resistivity of granulated loam as a function of moisture content and frequency.

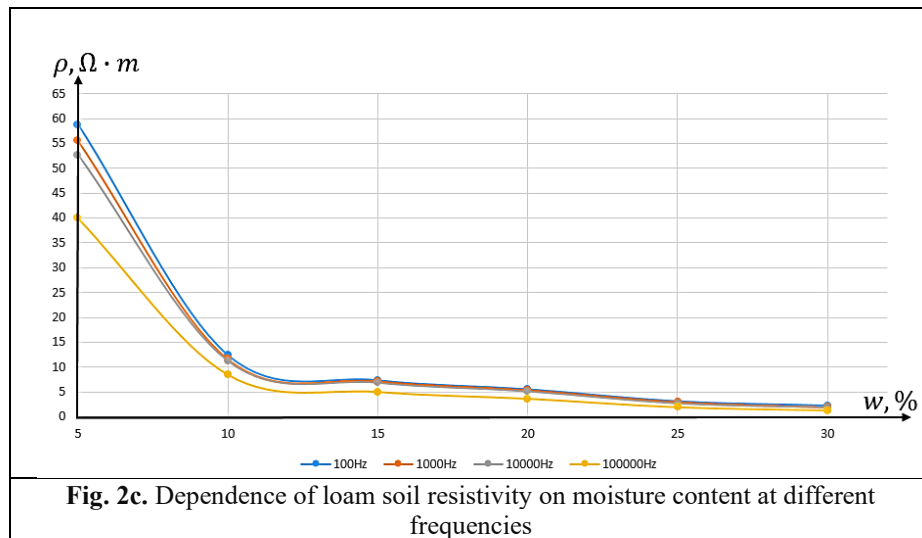


Fig. 2c. Dependence of loam soil resistivity on moisture content at different frequencies

According to the data (Fig. 2c), at low moisture levels the soil resistivity reaches high values (up to $60 \Omega \cdot m$); however, as moisture increases, a sharp decrease in ρ is observed down to a critical level of 12–13%, which is associated with the formation of continuous conductive channels in the pore space (percolation effect). In this region, a transition is recorded from a steep drop in resistivity to the establishment of a stable dependence: further increases in moisture are accompanied by an almost linear decrease in ρ , caused by the growth of pore fluid volume and the increased concentration of mobile ions.

Frequency analysis showed that increasing frequency also leads to a reduction in resistivity. At low frequencies (100–1 kHz), electrode polarization makes a significant contribution by forming a double electric layer at the “electrode–soil” interface. This frequency effect leads to an overestimation of the measured resistivity values. At higher frequencies (10–100 kHz), the influence of electrode polarization weakens, and resistivity is determined mainly by the ionic conductivity of the pore solution. For moisture contents above 20–25%, the resistivity curves obtained at different frequencies practically coincide. This indicates the dominant contribution of the ionic conductivity of the pore solution to the overall charge transport mechanism. Under these conditions, the influence of surface and polarization processes becomes negligible, and the soil conductivity is governed primarily by the concentration of dissolved salts and the degree of pore water saturation.

In order to identify the features of the conductivity mechanism, additional studies were carried out on the dependence of resistivity on moisture content for sand samples of different granulometries—fine-grained (Fig. 2d) and coarse-grained (Fig. 2g).

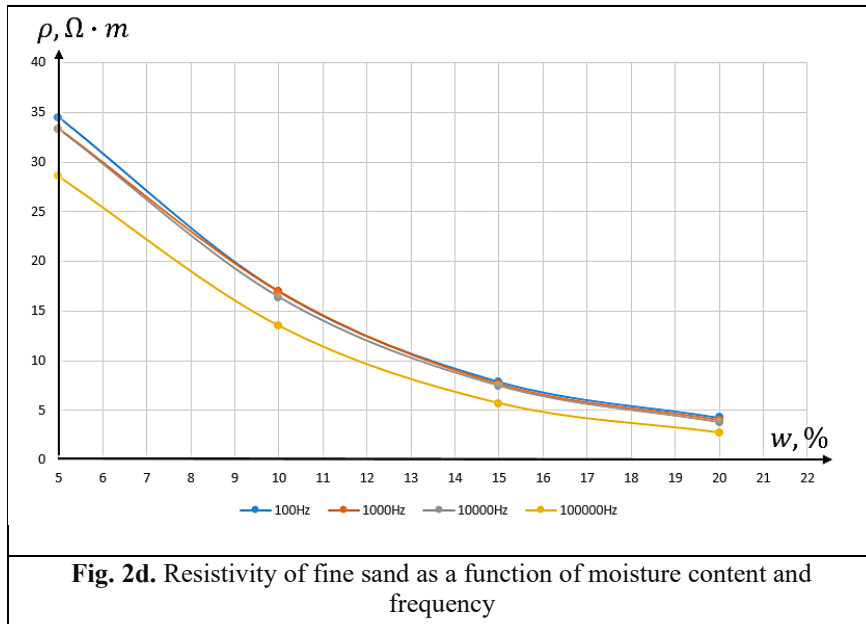
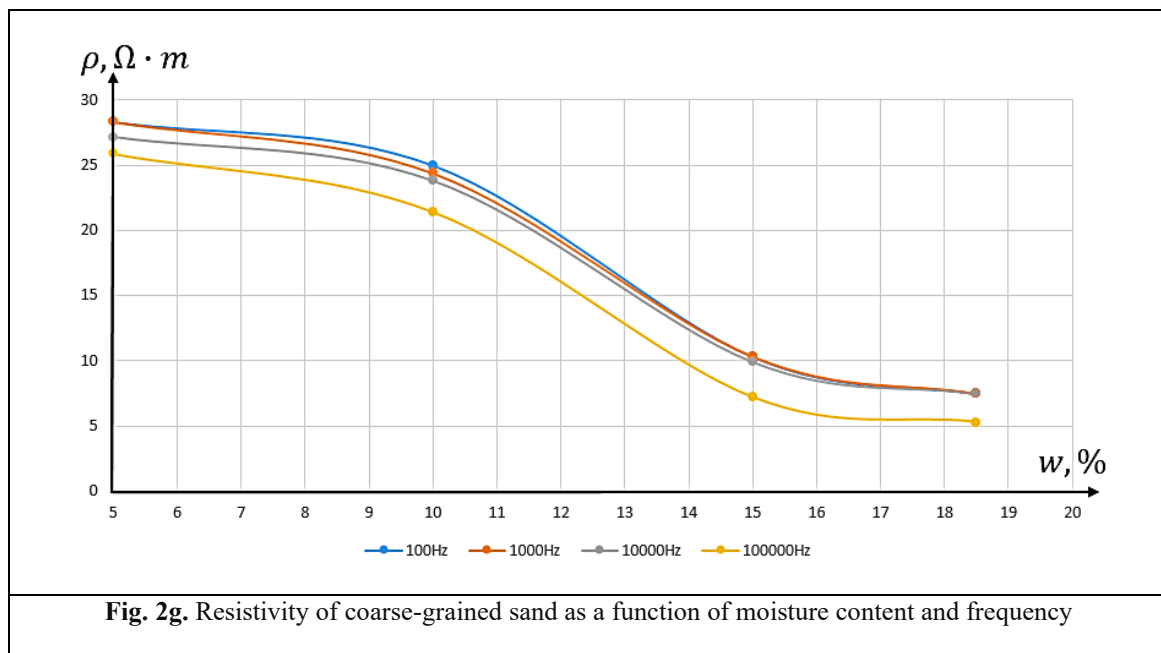


Figure 2d illustrates the monotonic decrease in soil resistivity with increasing moisture content. At low moisture levels (5–10%), ρ values reach 30–35 $\Omega \cdot m$; however, with an increase in moisture content to 15–20%, the resistivity decreases to 3–5 $\Omega \cdot m$. This pattern is explained by the percolation effect: as the amount of moisture increases, continuous conductive pathways are formed, enabling efficient ion transport. At a frequency of 100 Hz, the resistivity values are higher than at 10–100 kHz, which is explained by the contribution of electrode polarization and the formation of a double electric layer at the “electrode–soil” interface. As the frequency increases (10^3 – 10^5 Hz), the influence of surface effects diminishes, and the resistivity is determined mainly by the ionic conductivity of the solution. At moisture levels above 15–20%, the curves for all frequencies practically converge, indicating the dominance of the ionic charge transport mechanism. Under these conditions, surface and polarization processes become negligible, and soil conductivity is governed primarily by the concentration of dissolved salts and the degree of pore space saturation with moisture [37].



In Fig. 2g, the dependence is presented, from which it follows that in the moisture range of 5–10%, the soil resistivity lies within 25–30 $\Omega \cdot m$. A further increase in moisture content is accompanied by a gradual decrease in

Copyright to IJARSET www.ijarset.com 24348

ρ . In the range of 10–15%, the reduction in resistivity acquires a pronounced nonlinear character, which is associated with the formation of continuous current-conducting channels in the pore space (percolation effect). It is noticeable that at low moisture levels (5–8%), the differences between the curves obtained at different frequencies are insignificant. However, with a further increase in moisture, the influence of frequency becomes more pronounced. At 100 Hz, the resistivity is higher, which is explained by the effect of electrode polarization. With an increase in frequency (10–100 kHz), the contribution of polarization processes decreases, and the resistivity is determined mainly by the ionic conductivity of the pore solution. At moisture levels above 15–18%, the $\rho(\omega)$ dependencies obtained at different frequencies begin to converge. This indicates that at high moisture content, soil conductivity is governed primarily by the concentration of dissolved salts and the degree of pore saturation with water, while surface and polarization effects become secondary.

To compare the nature of the dependence of resistivity on moisture content, Fig. 3a presents the results obtained at a frequency of 100 Hz, which is equivalent to direct current measurement conditions.

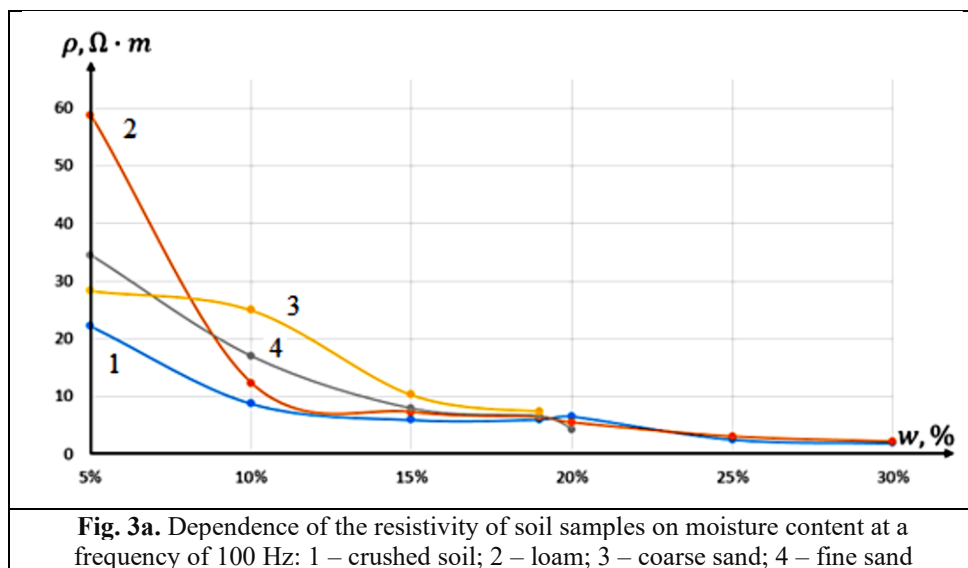


Fig. 3a. Dependence of the resistivity of soil samples on moisture content at a frequency of 100 Hz: 1 – crushed soil; 2 – loam; 3 – coarse sand; 4 – fine sand

As shown by the graphs (Fig. 3a), the dependencies of resistivity (ρ) on moisture content (ω) exhibit a complex character. The most pronounced changes are observed for granular soil and coarse-grained sand. In the low-moisture region, before the air pores become filled with water, these samples are characterized by high resistivity values. After reaching the threshold moisture level ($W \geq 12-15\%$), corresponding to the conditions of normal plant growth, the dependence $\rho = \rho(\omega)$ becomes almost linear: with further increases in moisture content, the resistivity decreases in an approximately linear manner. A similar pattern was previously noted in our earlier studies [13]. Analysis of the experimental data revealed a clear inverse relationship between soil moisture and its electrical resistivity. An increase in moisture is accompanied by a decrease in resistivity, which is associated with the formation of conductive channels in the pore space due to the presence of water. At the same time, the nature of resistivity variation is determined by the granulometric composition of the samples. Coarse sand demonstrates the highest resistivity values across the entire studied moisture range, which is explained by its low water-holding capacity and limited interparticle contact area that hinders the formation of stable conductive pathways. In contrast, fine sand is characterized by lower resistivity values due to its well-developed pore structure, capable of retaining more water and thus ensuring higher electrical conductivity. The most intense decrease in resistivity is observed for loam, which is associated with the high content of fine particles and clay minerals possessing a large specific surface area and strong water adsorption capacity, substantially enhancing the conductivity of the system. Crushed soil occupies an intermediate position: at low moisture content it shows relatively high resistivity, but as moisture increases, the reduction of this parameter occurs faster than in sandy samples, indicating a significant contribution of the fine fraction. The analysis showed that the dependence of resistivity on moisture content $\rho = \rho(\omega)$ for the studied samples retains its characteristic features up to frequencies of about 20 kHz. As an example, Fig. 3b presents a typical dependence of resistivity on moisture content.

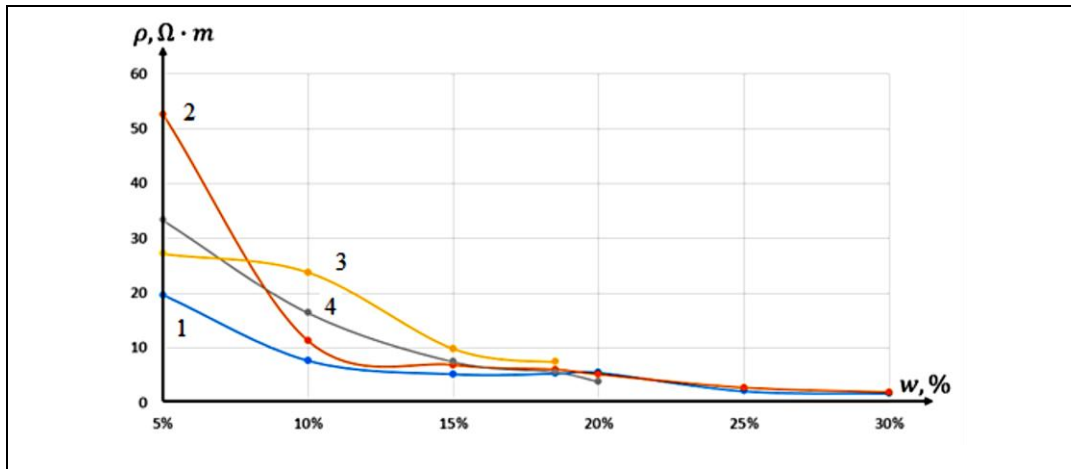


Fig. 3b. Dependence of the electrical resistivity of soil samples on moisture content at a frequency of 10 kHz: 1 – crushed soil; 2 – loam; 3 – coarse-grained sand; 4 – fine-grained sand

Both under direct current and at low-frequency alternating current, pronounced changes in resistivity are observed depending on moisture content, particularly for granular soil and coarse-grained sand. However, when the frequency exceeds 50 kHz, the character of the dependence $\rho = \rho(\omega)$ changes significantly. This effect is associated with the fact that at low frequencies the soil's conductivity is mainly determined by the ionic conductivity of the moisture filling the pore space, as well as by the formation of conductive channels [38]. With increasing frequency, the role of dielectric and polarization processes becomes more pronounced: dipole water molecules and ions can no longer reorient in phase with the external field, which leads to a reduced contribution of ionic conductivity and a change in the current transport mechanism. As a result, resistivity becomes less sensitive to variations in moisture content, and the dependence $\rho(\omega)$ takes on a different character.

As follows from Figure 3c, at high frequencies (for example, at $f = 100$ kHz), the most pronounced dependences of specific resistance on humidity are observed for fine-grained and coarse-grained sands.

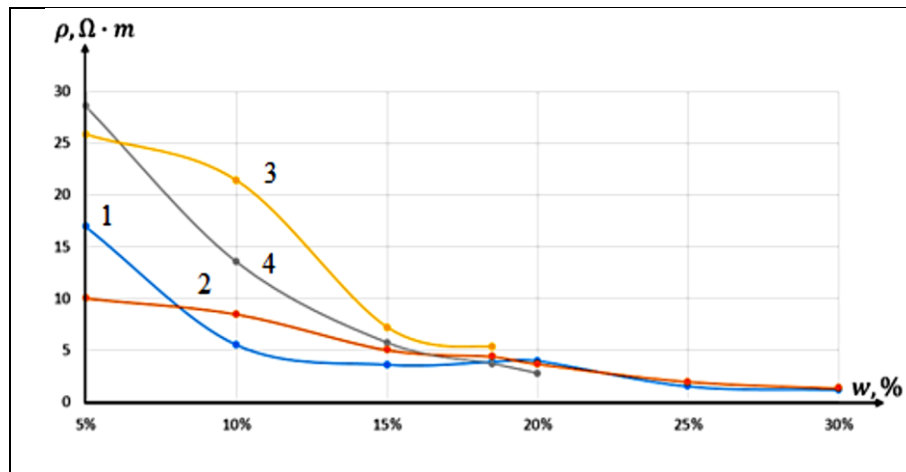


Fig. 3c. Dependence of the specific electrical resistance of soil samples on moisture content at a frequency of 100 kHz: 1 – finely ground soil; 2 – loam; 3 – coarse-grained sand; 4 – fine-grained sand.

The results obtained show that at this frequency, the nature of the resistance-humidity dependence differs significantly from that observed in the low-frequency range. While at frequencies of approximately 100 Hz and 10 kHz, the influence of the ionic conductivity of the moisture filling the pore space dominates, at 100 kHz, the contribution of capacitive and polarization effects increases. This is due to the fact that at high frequencies, dipole water molecules and ions are unable to follow changes in the external electric field [39], and the system's behavior begins to be determined by interfacial interactions at the solid particle-water-air boundaries.

The most pronounced dependences of $\rho(\omega)$ on moisture content were recorded for coarse-grained and fine-grained sand. This effect can be explained by the formation of intergranular microcapacitive structures in which water acts as a dielectric, and mineral particles act as electrodes [40]. As a result, the specific resistance of these samples is sensitive even to minor changes in moisture content. Loam, on the contrary, demonstrates a smoother dependence of resistance on moisture content. This is probably due to the high proportion of colloidal and clay particles, for which the contribution of ionic conductivity decreases at high frequencies, and capacitive effects are less pronounced due to the uneven distribution of moisture [41]. Crushed soil occupies an intermediate position: its resistance decreases with increasing moisture content, but the rate of this decrease is lower than that of sandy samples, which indicates the combined influence of the dispersed and sand fractions [42]. In the high-frequency region (100 kHz), the dependence of soil specific resistance on moisture content is determined not only by the volume of moisture, but also by the nature of its distribution in the pore space. For sandy samples, capacitive processes predominate, forming a sensitive dependence of ρ on ω , whereas for loamy soils and crushed samples this dependence is smoother.

Это приводит к возрастанию ёмкостной составляющей проводимости системы, при котором её сопротивление приобретает выраженную частотную зависимость и определяется выражением $X_c = 1/2\pi fC$ или в эквивалентной форме $X_c = 1/\omega C$.

This leads to an increase in the capacitive component of the system's conductivity, in which its resistance acquires a pronounced frequency dependence and is determined by the expression $X_c = 1/2\pi fC$ or in equivalent form $X_c = 1/\omega C$.

By determining the soil resistance in the frequency range up to 100 Hz, as well as at $f = (10-100)$ kHz, the value of the total resistance of the system can be expressed as [43]:

$$Z = \sqrt{R_0^2 + \left(\frac{1}{\omega C}\right)^2}, \tag{5}$$

where $\omega = 2\pi f$. Based on the dependence $Z = Z(f)$ or $R = R(f)$, the system capacitance was estimated. The difference between the values $Z_0 = R_0$ and Z can be designated as ΔR . The system capacitance was calculated using the formula:

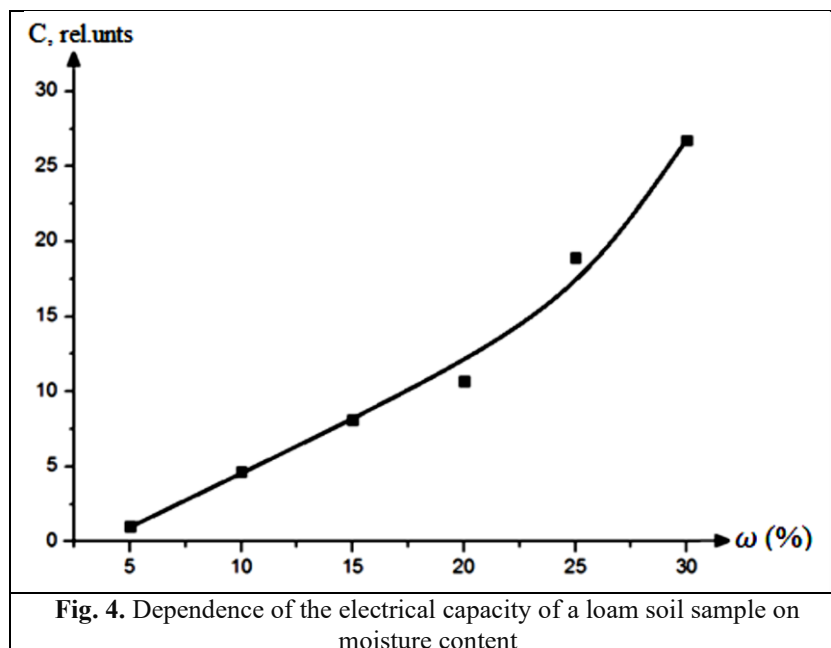
$$C = 1/2\pi f \sqrt{\Delta R^2 + 2\Delta R R_0} \tag{6}$$

For all the systems studied—crushed and granular soil, loam, fine-grained sand with a clay content of 25–30%, as well as coarse-grained sand—a clear pattern was revealed: with increasing moisture content, their capacitance increased. This effect is explained by the high relative dielectric permittivity of water and is associated with the formation of microcapacitor structures in the soil samples, which act as separate capacitive subsystems [44]. The summarized results of the calculated data for the various systems are presented in Table.

**Table
Estimated capacity of systems depending on their moisture level**

Humidity, %	Capacity of crushed soil, nF	Capacity of granular soil, nF	Capacity of fine-grained sand, nF	Capacity of coarse sand, nF
5	0.71	0.43	0.74	0.32
10	2.91	2.10	1.52	1.05
15	4.26	3.50	3.26	2.48
20	5.87	4.60	5.99	3.45 (18%)
25	9.40	8.14	-	-
30	13.3	11.5	-	-

For capacity measurements of sand samples, experiments were conducted at limited moisture contents, as water infiltrated up to 20% of fine-grained sand and up to 18% of coarse-grained sand when moisture content was calculated by weight. The results obtained correlate satisfactorily with directly measured capacity values; although the absolute values differed by coefficients, they were in the same order of magnitude. In both cases, an increase in the capacity of the systems with increasing moisture content was observed, approaching an exponential relationship (Fig. 4).



Processing of the experimental results (Fig. 4) showed that the capacity of the sample increases with increasing moisture content, and the dependence is close to exponential. This indicates that when the soil is moistened, its dielectric properties change significantly, in particular, the dielectric constant ϵ , which increases as the pore system is filled with water [45]. According to the information provided in the scientific literature [46, 47], the dielectric constant of the soil is conventionally divided into three ranges: arid conditions ($\epsilon < 10$), an optimal moisture range ($\epsilon = 40-70$), and a region of abundant moistening ($\epsilon \approx 80$). These ranges help explain the observed increase in capacity with increasing moisture: at low humidities, the capacity grows slowly, in the optimal range, a sharp increase is observed, and at high humidity, the upward trend slows down, approaching saturation. An important aspect is the structural organization of the loam. Finely dispersed and clay particles form a developed pore system, which, when moistened, promotes the formation of microcapacitor structures between the particles [48]. These structures provide a significant contribution to the overall capacity of the system and explain the exponential nature of the dependence.

The dependence of loam capacity on moisture content reflects the combined influence of water's dielectric properties and soil granulometric structure. The results highlight the importance of considering moisture content when assessing the electrical properties of loams and can be used to develop methods for remote monitoring of soil moisture and modeling electrophysical processes in soil systems.

IV. CONCLUSION

A comprehensive study of sierozem, loam, and sandy soils in the Tashkent and Syrdarya regions revealed a clear dependence of their electrophysical properties on moisture content, alternating current frequency, and particle size distribution. The main decrease in specific electrical resistance is observed in the early stages of wetting (up to 12-15%), when a continuous aqueous phase forms and charge transfer shifts from a surface to a bulk ionic mechanism [49,50].

An analysis of the resistivity of crushed soil, loam, and fine- and coarse-grained sands as a function of relative humidity under the influence of direct and alternating current (up to 100 kHz) confirmed these patterns. At frequencies above 50 kHz, a pronounced frequency dispersion of resistivity was revealed: its decrease is associated with the formation of water-saturated microlayers in the pore space, which act as capacitor-like structures. This effect is most pronounced in sands with a moisture content of 5-15%, emphasizing the importance of granulometric characteristics for soil electrical conductivity.

Furthermore, soil capacitance increases almost exponentially at elevated moisture levels, especially for granular soils (loams), indicating the formation of developed capacitive systems with water as the dielectric medium. These results demonstrate the high information content of capacitance measurements for assessing soil moisture.



The obtained data confirm the multi-mechanism nature of soil electrical conductivity and highlight the need for a comprehensive approach to its study. They can be used to refine soil electrical conductivity models and improve electrophysical methods for monitoring the moisture content and geotechnical properties of various soil types.

REFERENCES

1. Steven M. de Jong, Renée A. Heijnen, Wiebe Nijland and Mark van der Meijde. Monitoring Soil Moisture Dynamics Using Electrical Resistivity Tomography under Homogeneous Field Conditions. *Sensors* 2020, 20(18), 5313; <https://doi.org/10.3390/s20185313>.
2. A. D Adebisi, K. A. N Adiat & A. B Eluwole. Development of empirical models for analysis of subsoil agricultural parameters from resistivity measurement in a basement complex terrain. *Natural Resources Research. NRIAG Journal of Astronomy and Geophysics* (2020), 9(1):260-271. <https://doi.org/10.1080/20909977.2020.1732571>.
3. Zheng Fu, Philippe Ciais, Jean-Pierre Wigneron, Pierre Gentile, Andrew F. Feldman, David Makowski, Nicolas Viovy, Armen R. Kemanian, Daniel S. Goll, Paul C. Stoy, Iain Colin Prentice, Dan Yakir, Liyang Liu, Hongliang Ma, Xiaojun Li, Yuanyuan Huang, Kailiang Yu, Peng Zhu, Xing Li, Zaichun Zhu, Jinghui Lian & William K. Smith. Global critical soil moisture thresholds of plant water stress. *Nature Communications*, Vol.15, Article number: 4826 (2024). <https://doi.org/10.1038/s41467-024-49244-7>.
4. A.Q. Abdullayev, H.A. Arginboev, Abdullayev N.A. *Agrometeorology*. Tashkent: Uzgidromet, 2008. - pp. 168-187.
5. Mukhtar Iderawumi Abdullaheem, Hongjun Chen, Linze Li, Abiodun Yusuff Moshood, Wei Zhang, Yani Xiong, Yanyan Zhang, Lateef Bamidele Taiwo, Aitazaz A. Farooque, Jiandong Hu. Recent Advances in Dielectric Properties-Based Soil Water Content Measurements. *Nature Communications* (2024), 16(8), 1328. <https://doi.org/10.3390/rs16081328>.
6. Xingqian Xu, Haijun Wang, Xin Qu, Cheng Li, Bo Cai, Guangcan Peng. Study on the dielectric properties and dielectric constant model of laterite. *Front. Earth Sci.* (2022), Vol. 10. <https://doi.org/10.3389/feart.2022.1035692>.
7. Nimi Ann Vincent, R Shivashankar, K N Lokesh, Jinu Mary Jacob. Laboratory Electrical Resistivity Studies on Cement Stabilized Soil. *International Scholarly Research Notices* (2017) (1):1-15. <https://doi.org/10.1155/2017/8970153>.
8. Behdad Mofarraj Kouchaki, Michelle L. Bernhardt-Barry Corresponding, Clinton M. Wood, Tim Moody. A Laboratory Investigation of Factors Influencing the Electrical Resistivity of Different Soil Types. *Geotechnical Testing Journal* (2019), 42 (4): 829-853. <https://doi.org/10.1520/GTJ20170364>.
9. N.Yu. Sharibaev, A.Q. Ergashov, S.B. Fazliddinov, R.G. Ikramov, M.A. Yuldoshev, A.A. Abdulxayev, *Journal of Ovonic Research*. Vol.21, No.6, (2025). <https://doi.org/10.15251/JOR.2025.216.859>.
10. Sh.B. Utamuradova, Z.T. Azamatov, A.I. Popov, M.R. Bekchanova, M.A. Yuldoshev, and A.B. Bakhromov, *East Eur. J. Phys.* (3), 278 (2024), <https://doi.org/10.26565/2312-4334-2024-3-27>.
11. Bandar Alsharari, Andriy Olenko, Hossam Abuel-Naga. Modeling of Electrical Resistivity of Soil Based on Geotechnical Properties. *Expert Systems with Applications* (2020), vol. 141, 112966. <https://doi.org/10.1016/j.eswa.2019.112966>.
12. Fernando Ferreira Lima dos Santos, Daniel Marçal de Queiroz, Domingos Sárvio Magalhães Valente, Farzaneh Khorsandi, Guilherme de Moura Araújo. Analysis of Different Electric Current Frequencies in Soil Apparent Conductivity. *Journal of Biosystems Engineering* (2023), 48(5), Pp. 269-282. <https://doi.org/10.1007/s42853-023-00187-9>.
13. F. Turgunboev, K.A. Tursunmetov, Dependence of electrical properties of soil on its moisture content. *AGRO ILM*. Tashkent, 2020. No. 3. P. 64-65.
14. Xiao Jin, Wen Yang, Xiaoqing Gao, Zhenchao Li. Analysis and Modeling of the Complex Dielectric Constant of Bound Water with Application in Soil Microwave Remote Sensing. *Remote Sens.* (2020), 12(21), 3544. <https://doi.org/10.3390/rs12213544>.
15. Miles Dyck, Teruhito Miyamoto, Yukiyoshi Iwata, Koji Kameyama. Bound Water, Phase Configuration, and Dielectric Damping Effects on TDR-Measured Apparent Permittivity. *Vadose Zone Journal* (2019), vol. 18(1), Pp. 1-14. <https://doi.org/10.2136/vzj2019.03.0027>.
16. Humayun Kabir, Mohammad Jamal Khan, Graham Brodie, Dorin Gupta, Alexis Pang, Mohan V. Jacob. Measurement and modelling of soil dielectric properties as a function of soil class and moisture content. *Journal of Microwave Power and Electromagnetic Energy* (2020), 54(2):1-16. <https://doi.org/10.1080/08327823.2020.1714103>.
17. Timothy B. Wilson, John Kochendorfer, Howard J. Diamond, Tilden P. Meyers, Mark Hall, Temple R. Lee, Rick D. Saylor, Praveena Krishnan, Ronald D. Leeper, Michael A. Palecki. Evaluation of soil water content and bulk electrical conductivity across the U.S. Climate Reference Network using two electromagnetic sensors. *Vadose Zone Journal* (2024), vol. 23(4), e20336. <https://doi.org/10.1002/vzj2.20336>.
18. Mina Zamanian, Natnael Asfaw, Prakash Chavda, Mohsen Shahandashti. Deep Learning for Exploring the Relationship Between Geotechnical Properties and Electrical Resistivities. *Transportation Research Record Journal of the Transportation Research Board* (2024), 2678(1). <https://doi.org/10.1177/0361198124123491>.
19. José Paulo Molini, Gustavo Di Chiacchio Faulin. Spatial and temporal variability of soil electrical conductivity related to soil moisture. *Agricultural Engineering. Sci. agric. (Piracicaba, Braz.)* (2013), 70 (1). <https://doi.org/10.1590/S0103-90162013000100001>.
20. Paul W.J. Glover. Archie's law – a reappraisal. *Solid Earth*, 2016, 7(4):1157–1169. <https://doi.org/10.5194/se-7-1157-2016>.
21. Md Jobair Bin Alam, Ashish Gunda and Asif Ahmed. Machine Learning Approach to Model Soil Resistivity Using Field Instrumentation Data. *Geotechnics* (2025), 5(1), 5. <https://doi.org/10.3390/geotechnics5010005>.
22. F.A. Giyasova, A.Z. Rakhmatov, Kh.N. Bakhronov, M.A. Yuldoshev, F.A. Giyasov, A.N. Olimov, N.A. Sattarov, *East Eur. J. Phys.* 4, 397 (2025). <https://doi.org/10.26565/2312-4334-2025-4-38>.
23. J. Carlos Santamarina, A. Klein & Moheb A. Fam. Soils and waves: Particulate materials behavior, characterization and process monitoring. *Journal of Soils and Sediments* (2001), 1(2):130-130. <https://doi.org/10.1007/BF02987719>.
24. Wunderlich, Tina, Petersen, Hauke, Al Hagrey, Said Attia and Rabbel, Wolfgang. Pedophysical Models for Resistivity and Permittivity of Partially Water-Saturated Soils. *Pedophysical Models for Resistivity and Permittivity of Partially Water-Saturated Soils. Vadose Zone Journal* (2013), 12 (4). <https://doi.org/10.2136/vzj2013.01.0023>.
25. F.A. Giyasova and M.A. Yuldoshev. Investigation of temporal characteristics of photosensitive heterostructures based on gallium arsenide and silicon. *Chalcogenide Letters* (2025), 22(2), 123-129. <https://doi.org/10.15251/CL.2025.222.123>.
26. A.J. Merritt, J.E. Chambers, P.B. Wilkinson, L.J. West, W. Murphy, D. Gunn, S. Uhlemann. Measurement and modelling of moisture-electrical resistivity relationship of fine-grained unsaturated soils and electrical anisotropy. *Journal of Applied Geophysics* (2016), vol. 124, Pp. 155-165. <https://doi.org/10.1016/j.jappgeo.2015.11.005>.



27. A. Revil. Effective conductivity and permittivity of unsaturated porous materials in the frequency range 1 mHz-1GHz. *Water Resources Research* (2013), 49(1):306-327. <https://doi.org/10.1029/2012WR012700>.
28. Fatima Zohra-Hadjadj, Nadia Laredj, Mustapha Maliki, Hanifi Missoum, Karim Bendani. Laboratory evaluation of soil geotechnical properties via electrical conductivity Evaluación de laboratorio de las propiedades geotécnicas del suelo mediante conductividad eléctrica. *Revista Facultad de Ingeniería* (2019), 90(90):101-112. <https://doi.org/10.17533/udea.redin.n90a11>.
29. Ben Ishai, Paul, Talary, Mark S., Caduff, Andreas, Levy, Evgeniya, Feldman, Yuri. Electrode polarization in dielectric measurements: a review. *Measurement Science and Technology*, Volume 24, Issue 10, article id. 102001 (2013). <https://doi.org/10.1088/0957-0233/24/10/102001>.
30. J R Yusupov, M Ehrhardt, Kh Sh Matyokubov and D U Matrasulov. Driven transparent quantum graphs. *Phys. Scr.* (2025), 100 075224. <https://doi.org/10.1088/1402-4896/ade014>.
31. Odil Yunusov, Bobur Turimov, Yokubjon Khamroev, Sulton Usanov, Farkhodjon Turaev, Markhabo Kuliyeva. Charged Zipoy–Voorhees metric in string theory. *Annals of Physics* (2025), vol. 481, 170151. <https://doi.org/10.1016/j.aop.2025.170151>.
32. Hu Zeng, Qianli Zhang, Cui Du, Jie Liu and Yilin Li. Quantitative Relationship Between Electrical Resistivity and Water Content in Unsaturated Loess: Theoretical Model and ERT Imaging Verification. *Geosciences* (2025), 15(8), 302. <https://doi.org/10.3390/geosciences15080302>.
33. M. Loewer, T. Günther, J. Igel, S. Kruschwitz, T. Martin, N. Wagner. Ultra-broad-band electrical spectroscopy of soils and sediments-a combined permittivity and conductivity model. *Geophysical Journal International* (2017), vol. 210, Issue 3, Pp. 1360–1373. <https://doi.org/10.1093/gji/ggx242>.
34. F.A. Giyasova, Kh.N. Bakhronov, M.A. Yuldoshev, I.B. Sapaev, R.G. Ikramov, F.A. Giyasov, M.R. Bekchanova, M.M. Qaxxarov, H.O Abdullayev, *East Eur. J. Phys.* 4, 461 (2025). <https://doi.org/10.26565/2312-4334-2025-4-47>.
35. Kornkanok Sangprasat, Avirut Puttiwongrak and Shinya Inazumi. Review of Correlations Between Soil Electrical Resistivity and Geotechnical Properties. *Geosciences* (2025), 15(5), 166. <https://doi.org/10.3390/geosciences15050166>.
36. Kh. Yu. Rakhimov, H. T. Yusupov, Sh. R. Nurmatov, Andrey Chaves, G. R. Berdiyrov. Wave-packet rectification in graphene with alternating circular electrostatic potential barriers. *J. Appl. Phys.* (2025), 137, 144302. <https://doi.org/10.1063/5.0250401>.
37. S. Nandi and C. Vipulanandan. Effect of Moisture content on the Electrical Resistivity of Sand. *CIGMAT-2021 Conference & Exhibition, II-5 – II-9*.
38. Federico Delfino, Renato Procopio, Mansueto Rossi, Farhad Rachidi. Influence of frequency-dependent soil electrical parameters on the evaluation of lightning electromagnetic fields in air and underground. *Journal of Geophysical Research Atmospheres* (2009), 114(D11). <https://doi.org/10.1029/2008JD011127>.
39. Farizal Hakiki, Chih-Ping Lin. Electrical Conductivity and Permittivity of Porous Media: Origin, Measurements, and Implications. *ACS Measurement Science Au* (2025). <https://doi.org/10.1021/acsmesuresciau.5c00070>.
40. Thomas Kremer, Myriam Schmutz, Philippe Leroy, Pierre Agrinier, Alexis Mainault. Modeling the spectral induced polarization response of water-saturated sands in the intermediate frequency range (102-105 Hz) using mechanistic and empirical approaches. *Geophysical Journal International* (2016), 207(2): ggw 334. <https://doi.org/10.1093/gji/ggw334>.
41. Tina Wunderlich, Hauke Petersen, Said Attia al Hagrey, Wolfgang Rabbel. Pedophysical Models for Resistivity and Permittivity of Partially Water-Saturated Soils. *Vadose Zone Journal* (2013), 12(4). <https://doi.org/10.2136/vzj2013.01.0023>.
42. Muataz M. Al-Moadhen, Barry G. Clarke, Xiaohui Chen. Electrical conductivity of sand-clay mixtures. *Environmental Geotechnics* (2024), 11(8):615-628. <https://doi.org/10.1680/jenge.21.00048/>
43. Orjan G. Martinsen, Sverre Grimnes *Bioimpedance and Bioelectricity Basics*. 2nd Edition. Academic Press (2011), 585 p.
44. S.F. Samadov, N.V.M. Trung, A.A. Sidorin, S.I. Ibragimova, S.H. Jabarov, M.A. Yuldoshev, O.S. Orlov, Y.I. Aliyev, *Micro and Nanostructures* 209 (2026) 208451, (2026). <https://doi.org/10.1016/j.micrna.2025.208451>.
45. R. Stenger, T. Wöhling, G. F. Barkle and A. Wall. Relationship between dielectric permittivity and water content for vadose zone materials of volcanic origin. *Australian Journal of Soil Research* (2007), 45(4):299-309. <https://doi.org/10.1071/SR06172>.
46. D.A. Robinson, S.B. Jones, J. M. Wraith, D. Or, S. P. Friedman. A Review of Advances in Dielectric and Electrical Conductivity Measurement in Soils Using Time Domain Reflectometry. *Vadose Zone Journal* (2003), 2:444-475. <https://doi.org/10.2136/vzj2003.4440>.
47. Stuart. O. Nelson. Dielectric Properties of Agricultural Products: Measurements and Applications. *IEEE Transactions on Electrical Insulation* (1991), 26(5):845 – 869.
48. Xicai Pan, Yudi Han, Kwok Pan Chun, Jiabao Zhang, Donghao Ma, Hongkai Gao. On the laboratory calibration of dielectric permittivity models for agricultural soils: Effect of systematic porosity variation. *Vadose Zone Journal* (2021), 20(1). <https://doi.org/10.1002/vzj2.20096>.
49. Sh.B. Utamuradova, F.A. Giyasova, K.N. Bakhronov, M.A. Yuldoshev, M.R. Bekchanova, B. Ismatov. Current Transfer Mechanism in a Thin-Based Heterosystem Based on A²B⁶ Compounds. *East European Journal of Physics*. 3, 325 (2025), <https://doi.org/10.26565/2312-4334-2025-3-31>.
50. Sh. B. Utamuradova, F. A. Giyasova, M. S. Paizullakhanov, S. Yu. Gerasimenko, M. A. Yuldoshev, S. R. Boydedayev, M. R. Bekchanova. Investigation of the functional capability. *Chalcogenide Letters*. Vol. 22, No. 8, August 2025, p. 753-764. <https://doi.org/10.15251/CL.2025.228.753>.

AUTHOR'S BIOGRAPHY

Full name	Farxod Turgunboev
Science degree	PhD
Academic rank	Assistant Professor
Institution	National University of Uzbekistan named after Mirzo Ulugbek, Tashkent, Uzbekistan



Full name	Kamiljan A. Tursunmetov
Science degree	DSc
Academic rank	Professor
Institution	National University of Uzbekistan named after Mirzo Ulugbek, Tashkent, Uzbekistan

Full name	Feruza A. Giyasova
Science degree	DSc
Academic rank	Professor
Institution	Kimyo International University in Tashkent, Uzbekistan

Full name	Murodjon A. Yuldoshev
Science degree	PhD
Academic rank	Assistant Professor
Institution	Turan International University, Namangan, Uzbekistan

Full name	Farkhod A. Giyasov
Science degree	-
Academic rank	Head teacher
Institution	Kimyo International University in Tashkent, Uzbekistan

Full name	Azimjon A. Abduvakhobov
Science degree	-
Academic rank	Head teacher
Institution	Kimyo International University in Tashkent, Uzbekistan

Full name	Alisher A. Mamadaliyev
Science degree	-
Academic rank	Master's student
Institution	Kimyo International University in Tashkent, Uzbekistan